

2D-3D multiscale modelling of inhomogeneous plasma amplifiers

Pablo Martínez Gil ^{a,b}, José A. Moreno ^{a,b}, Jorge Álvarez ^a, Antonio Luque ^a, Francisco Ribas ^a,
Marina Ruiz ^a, Eduardo Oliva ^{*a,b}

^aDepartamento de Ingeniería Energética, E.T.S.I. Industriales, Universidad Politécnica de Madrid, Madrid, Spain; ^bInstituto de Fusión Nuclear “Guillermo Velarde”, E.T.S.I. Industriales, Universidad Politécnica de Madrid, Spain.

ABSTRACT

Optical field ionized (OFI) plasma amplifiers have recently demonstrated sub-picosecond pulses when seeded with high order harmonics. In addition to this, the intensity and phase profile of the amplified harmonic beams carry information about possible plasma inhomogeneities (electron density, lasing ion abundance) that may appear in the amplifier. 1D and 3D modelling has played a fundamental role in these results and it will be required to support present and future experiments. This modelling involves different physical processes and time-scales, from the nanoseconds (hydrodynamics) to the picoseconds (atomic physics) and femtoseconds (dynamics of the amplified beam). Here we briefly present the different codes that have been coupled to fully model this process, from the creation of the plasma to the amplification of XUV and soft X-ray,s and show how this framework can be applied to study the impact of plasma inhomogeneities in the intensity and phase profile of the amplified beam.

Keywords: plasma based soft X-ray lasers, high order harmonics, plasma hydrodynamics, Maxwell-Bloch equations, Particle-In-Cell, plasma physics.

1. INTRODUCTION

Plasma based soft X-ray lasers (PBSXRL) seeded with high order harmonics (HOH) are a promising source of coherent XUV and soft X-ray beams. Different lasing schemes to create a plasma amplifier have already been demonstrated [1-6] and used to amplify HOH [7-10]. Indeed, PBSXRL have demonstrated hundreds of femtosecond pulses [10] and are expected to deliver sub-picosecond, miliJoule and fully coherent soft X-ray beams [11-13].

Among all these different kind of plasma based lasers, optical field ionized (OFI) amplifiers have been used to demonstrate several key steps in the development of these sources: the first saturated amplification of high order harmonics in a plasma [7], the amplification of circularly polarized beams [14], the delivery of sub-picosecond pulses when seeding at high density [10] and the characterization of the intensity and phase profile of the amplified beam [15].

These recent advances required the use of advanced experimental and modelling techniques in order to interpret the results and unveil the dynamics of the plasma and the amplification process. In this article we will present the computational tools we used to fully model these multiscale, multiphysics experiments, from the hydrodynamics of the plasma (with characteristic time of the order of nanoseconds) to electron-ion collisions and atomic physics (picoseconds) and the dynamics of amplification of HOH (tens of femtoseconds).

The layout of the article is as follows. We briefly explain the methodology followed to model plasma based seeded soft X-ray lasers based on the OFI scheme and using Nickel-like Krypton as lasing ion. The different codes used will be described in each subsection. Afterwards, we will show some preliminary results on the impact of plasma inhomogeneities, that appear mainly due to overionization, in the resulting amplified beam. These inhomogeneities (which are an excess of electrons and a low abundance of lasing ions in some regions of the plasma) impact both the intensity and phase of the amplified beam and can thus be diagnosed by comparing experimental results and modelling. Finally, some conclusions and future prospects will be given.

*eduardo.oliva@upm.es

2. METHODOLOGY

In this section we will explain the computational tools we use to model the amplification of HOH in plasma based soft X-ray lasers. We use ARWEN [16,17] to model the creation and subsequent hydrodynamic evolution of the plasma. The data obtained from ARWEN (electron density profile, mean ionization) is used as initial condition in Particle-In-Cell (PIC) codes to model the propagation of the intense infrared (IR) pump laser through the millimeter-sized plasma amplifier. We have used the PIC codes WAKE-EP [18,19] and FBPIC [20]. The propagated IR beam along the resulting electron density profile and ionization abundance are fed to atomic codes, that compute collisional rates and the lasing ion's level populations, and Maxwell-Bloch codes that compute the amplification of HOH. We use the collisional-radiative code OFIKinRad [21] to compute the atomic quantities that, along electron density and ionization abundance, are fed to our Maxwell-Bloch codes, 1D-DeepOne [22] and 3D Dagon [23]. These codes allow to model the spatio-temporal amplification dynamics of the seeded HOH.

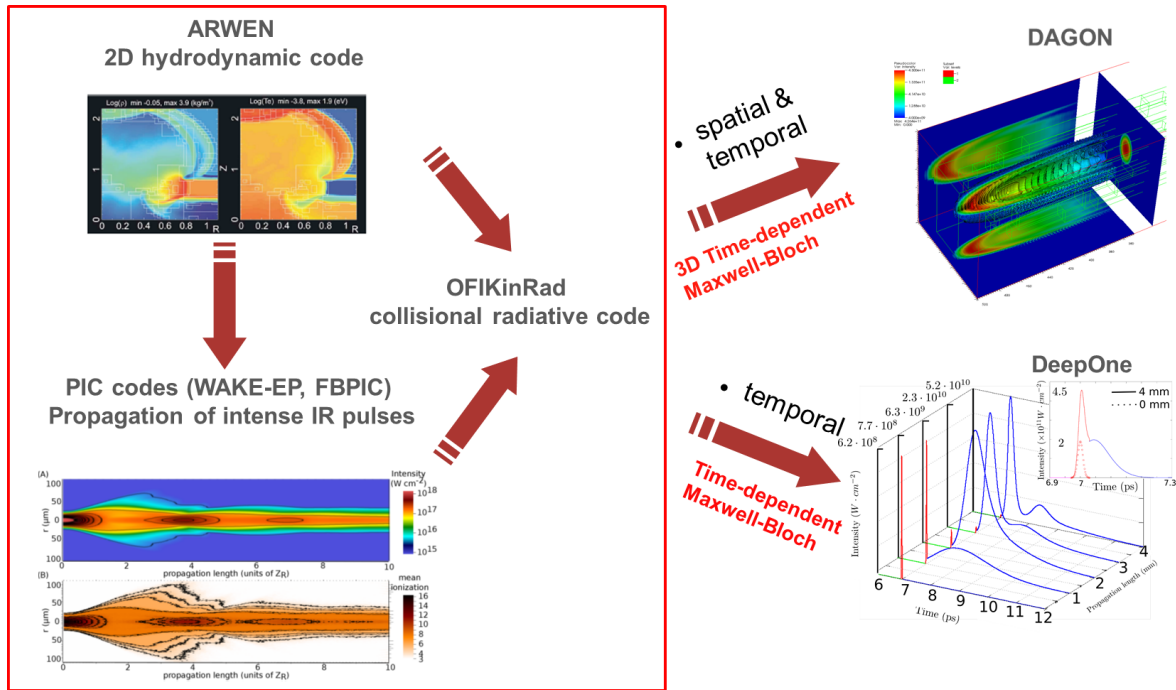


Figure 1. Scheme of the different codes used to model OFI plasma amplifiers seeded with high order harmonics. Red arrows show the different couplings between codes (i.e. some of the data output is used as input and/or initial condition).

2.1 Plasma hydrodynamics

While plasma hydrodynamics plays a crucial role in the evolution and dynamics of plasma amplifiers created from solid targets, it might be neglected when modelling collisionally pumped OFI plasma amplifiers. This kind of amplifiers are created and pumped by the propagation of an intense IR laser through a millimeter-sized gas medium (Kr, for example). The intense electric field of the laser ionizes the atoms, creates the plasma and accelerates the free electrons, heating them. These electrons collide with the ions pumping the population inversion. All the processes involved have characteristic times of the order of picoseconds or smaller, while the plasma evolves hydrodynamically in nanosecond time scales. Thus, it is possible to neglect this process and assume fixed plasma properties.

However, there is a kind of OFI amplifier that requires to take into account plasma hydrodynamics. Sub-picosecond amplified pulses can be achieved in OFI amplifiers when the electron density is high enough to overionize the lasing ion (Kr^{8+} in this case) effectively shutting temporally the amplification and thus reducing the duration of the amplified pulse [10]. However, the electron density required ($\sim 10^{20} \text{ cm}^{-3}$) hinders the propagation of the IR pump pulse. It is thus necessary to create a plasma waveguide [24] by letting the plasma expand, resulting in an increasing parabolic density

profile that allows the IR pulse to propagate throughout all the amplifier length [25,26]. The plasma creation and subsequent evolution towards this waveguide shape or plasma channel has been modelled with ARWEN [16,17]

ARWEN is a 2D adaptive mesh refinement (AMR) radiative hydrodynamics code. Plasma hydrodynamics is solved using an unsplit second-order Godunov method with multi-material capabilities. Electron heat conduction is modelled using flux-limited diffusion while radiative transfer uses a multi-group discrete-ordinate (S_n) synthetically accelerated transport method. The AMR paradigm is included using the BoxLib package [27]. Equations of state and opacities are provided in tabular form. They are based in the quotidian EOS [28] fitted to experimental data and the BigBART code [29,30] respectively.

The formation and evolution of the plasma waveguide along 4 ns was studied with ARWEN [26]. The results compared well with experimental data, capturing the radial expansion velocity and the resulting parabolic density profile. However, the electron density and mean ionization were overestimated by a factor of approximately two. This problem might come from the local thermodynamic equilibrium assumption when computing the mean ionization, concluding that a time-dependent computation of the transient ionization process would improve the accuracy of the model.

2.2 Propagation of intense IR pulses through plasmas

In this kind of OFI amplifiers, whether high or low density, an intense IR pulse propagates through a millimeter or even centimeter size plasma (a plasma waveguide in the former case or a low density plasma created by the head of the pulse in the latter). Since this IR beam creates the lasing ion and heats the electrons so they can collisionally pump the amplifier it is crucial to understand and control its propagation throughout the amplifier. For this task we have used the particle-in-cell (PIC) codes WAKE-EP [18,19] and FBPIC [20].

The propagation of an intense ($I \sim 10^{18} \text{ Wcm}^{-2}$) IR pulse through low density plasmas was modelled with the 2D axisymmetric code WAKE-EP. It is a fully relativistic, nonlinear particle code suited to model the interaction of short pulses with under-dense plasmas since it takes advantage of several approximations: electron motion is separated into a slowly varying component (due to the ponderomotive potential) and a fast quiver motion (due to the electric field oscillation); the quasi-static approximation, which assumes that the electrons travelling through the laser pulse are faster than the deformation of the laser beam and finally the laser propagation is computed using the envelope approximation. The radial electron density profile is approximated as a parabola and fed as an initial condition to the code.

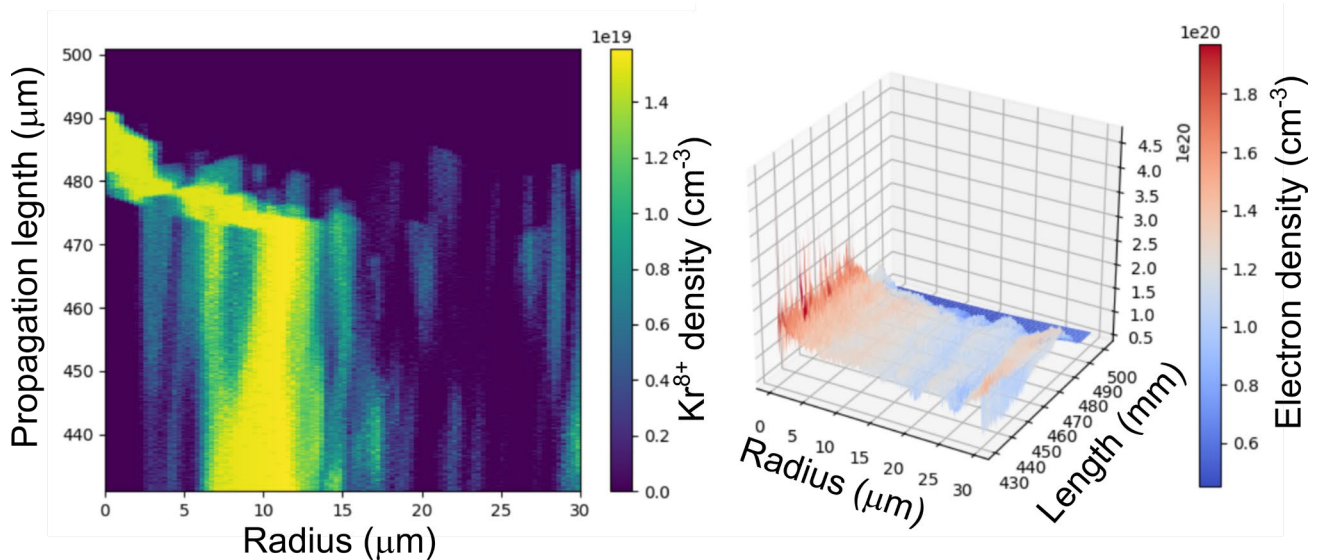


Figure 2. (left) Lasing ion (Kr^{8+}) density (cm^{-3}) at the entrance of a high density plasma waveguide (430-500 μm). The central region (0-5 μm) lacks lasing ion since the intensity of the laser pulse is high enough to overionize it. (right) Electron density (cm^{-3}) profile in the same region of the amplifier.

The modelization of low density plasma waveguides unveiled an oscillatory defocusing-focusing mechanism, similar to filamentation dynamics, in which ionization induced refraction defocus the laser beam while the radial density profile

and relativistic effects focus the beam. The intensity propagated allowed the existence of the lasing ion along all the length of the amplifier although overionized regions appeared in several parts of the amplifier.

Due to the approximations implemented in WAKE-EP, this code is not adequate to model dense plasmas. For this kind of plasma we have used FBPIC [20]. FBPIC (Fourier-Bessel Particle-In-Cell) is a PIC code especially suited to model plasmas with cylindrical symmetry, as the aforementioned plasma waveguide, thanks to its cylindrical grid with azimuthal decomposition. Maxwell equations are solved in the spectral space, avoiding artifacts. In addition to this, FBPIC has parallel and CUDA capabilities, ensuring reduced costs in terms of computation time. Unlike WAKE-EP, FBPIC does not require the assumption of an under-dense plasma and thus it is well suited to model the propagation of intense IR pulses through dense plasma waveguides.

The modelling shows similar results as the low density case. The IR pulse propagates throughout all the amplifier creating the lasing ion. However, its abundance is neither radially nor longitudinally homogeneous. The region in which the lasing ion is predominant reduces its radial width with the propagation length. Moreover, overionized regions appear in the amplifier. The existence and impact of these regions on the amplified beam has been recently confirmed [15].

2.3 Atomic physics modelling

As aforementioned, the IR pump pulse creates the lasing ions by optical field ionization. The resulting electrons, which are non-maxwellian, relax to a Maxwell energy distribution function (EDF) by electron-electron collisions. In addition to this, electron-ion collisions excite the lasing ions creating a population inversion between two excited levels and further ionizes them. All these processes are modelled using the code OFIKinRad [21]. The propagated intensity as given by PIC simulations along the mean ionization and electron density given by hydrodynamic modelling are used as initial conditions. The evolution of the EDF is obtained by solving a Fokker-Planck equation and rate equations are solved to compute the populations of the atomic levels of interest. From this modelling, the temporal evolution of the electron density, electron-ion collision frequency, collisional (de)excitation rates and level populations are extracted to be fed to our Maxwell-Bloch model.

2.4 Amplification of XUV and soft X-rays in plasmas

The amplification of XUV and soft X-rays in this kind of plasma amplifiers is modelled solving Maxwell-Bloch equations with our codes 1D-DeepOne [22] and 3D Dagon [23]. These codes solve the Maxwell wave equation for the electric field with paraxial and slowly varying envelope approximations. There is a constitutive relationship for the polarization that includes spontaneous emission (via a stochastic source term), collisional depolarization and amplification/absorption. Finally, a simplified atomic model, fed with data from more complete atomic physics codes like OFIKinRad, is solved to compute the populations of the levels involved in the lasing transition. With these codes the full 4D spatio-temporal dynamics of amplification is retrieved, allowing us to retrieve the intensity, wavefront, duration, energy, etc ... of the amplified beam.

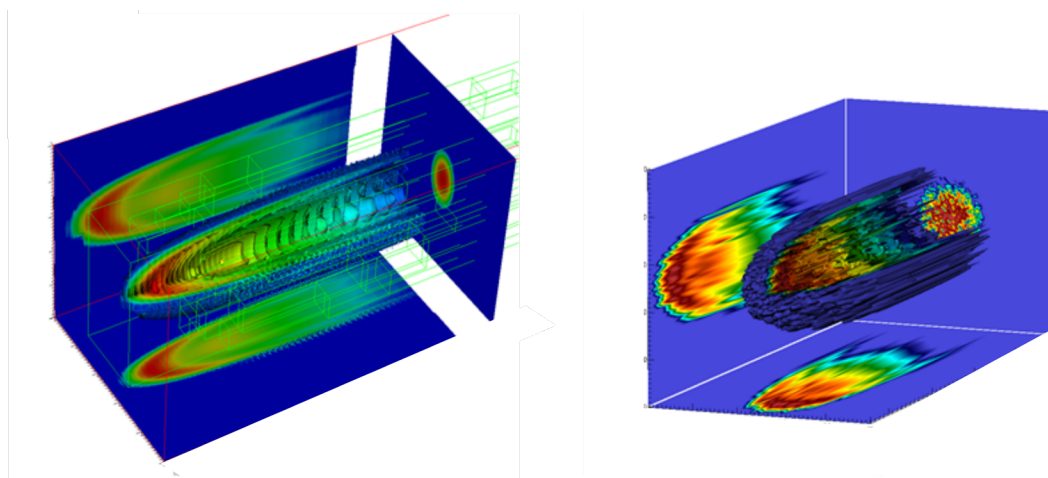


Figure 3. (left) Spatio-temporal structure of an amplified high order harmonic as modelled with Dagon. The complex temporal structure can be seen in its central part. (right) Spatio-temporal structure of amplified spontaneous emission (ASE) as modelled with Dagon. Its stochastic nature is clearly captured by the model.

3. APPLICATION OF THE MODELLING FRAMEWORK TO INHOMOGENEOUS PLASMA WAVEGUIDES

In this section we will show an example of application of the modelling framework described in the previous section. This example consists on a Krypton optical field ionized dense plasma amplifier [10, 15]. A sequence of two infrared pulses creates a low ionized plasma that expands hydrodynamically, resulting in a plasma waveguide with an increasing parabolic radial density profile. An intense ($I > 10^{18} \text{ Wcm}^{-2}$) infrared pulse propagates through this waveguide, creating the lasing ion (Kr^{8+}) by optical field ionization. The complex propagation process, as unveiled by PIC simulations, creates overionized regions lacking lasing ion and having an excess of electron density (which can be roughly approximated as a decreasing parabola [25]). In the regions where the lasing ion is abundant enough, strong gain appears, with a duration shorter than one picosecond, as shown in figure 4 left panel.

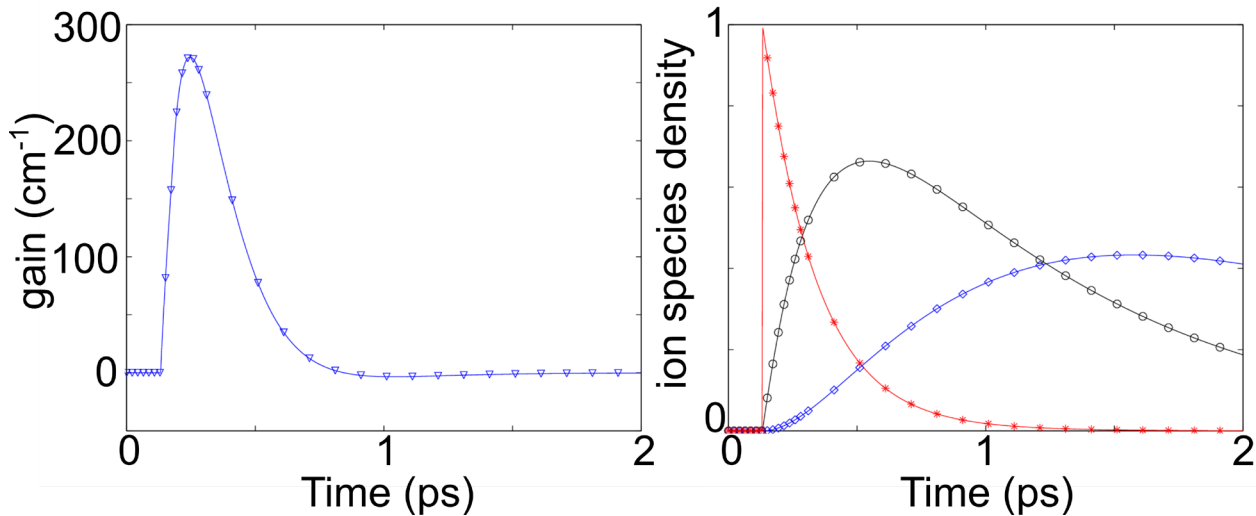


Figure 4. (left) Gain temporal dynamics and (right) temporal variation of the relative density of Kr^{8+} (red stars), Kr^{9+} (black circles) and Kr^{10+} (blue diamonds).

As expected, the gain temporal profile is linked to the abundance of the lasing ion Kr^{8+} . This ion is created almost instantly by the IR pump laser, since the characteristic time of optical field ionization is of the order of femtoseconds. The gain does not rise so steeply, as it is created after the lasing ion by electron collisional excitation. The relatively high electron density achieved in this amplifier ($n_e > 10^{20} \text{ cm}^{-3}$) creates the population inversion in hundreds of femtoseconds but also ionizes further the lasing ion, shown in figure 4 right panel. This depletion of the lasing ion due to collisional ionization, the so-called collisional ionization gating [10] quenches the gain in hundreds of femtoseconds, resulting in a strong but short-lived gain expected to efficiently amplify HOH beams maintaining a sub-picosecond duration.

The lasing ion abundance and electron density profile is introduced in our 3D Maxwell-Bloch model Dagon in order to study the impact of these inhomogeneities in the amplified beam intensity and phase profiles. Figure 5 shows the inhomogeneous plasma waveguide modelled.

Since the intensity of the IR pump pulse is the highest at the entrance of the plasma waveguide, this region is strongly overionized. Amplification in this region is negligible due to the low abundance of lasing ions and thus the effect of this region in the amplified beam is a modulation of its phase profile, the higher the density the stronger the modulation is.

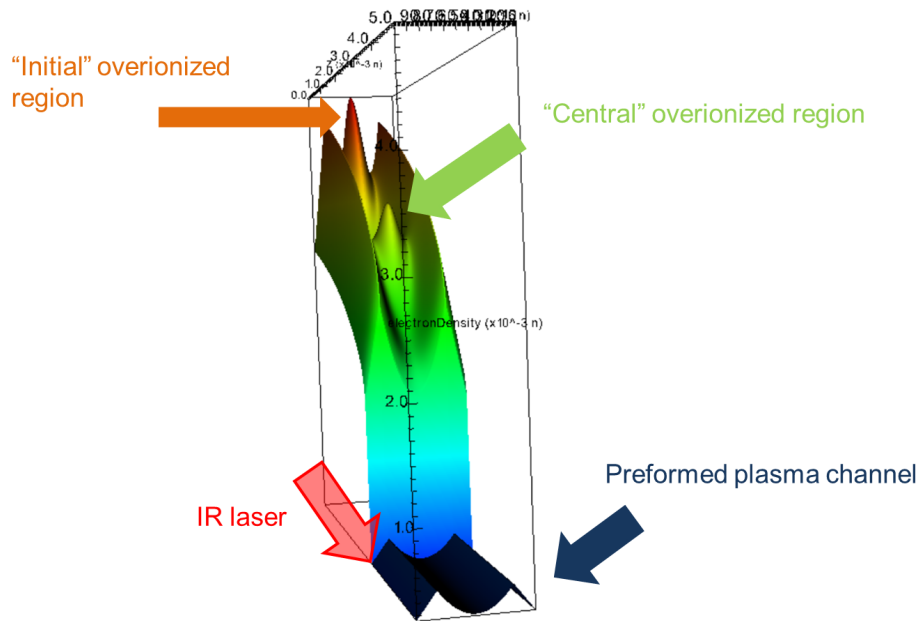


Figure 5. Electron density inhomogeneities in the plasma waveguide. The waveguide through which the IR pulse propagates is denoted as “preformed plasma channel”. The IR pulse propagates through it, increasing the ionization and thus the electron density. Two overionized regions are depicted here.

The second region, named central overionized region in figure 5, appears due to focusing effects that increase the propagated IR intensity until it attains values that can further ionize the lasing ion. This central region differs from the initial one in two aspects. First, the intensity of the IR laser is lower and thus the electron density peak and the ionization is smaller than in the initial regions. Second, the lasing ion is depleted in a small radius region where the IR intensity is high enough to ionize all lasing ions but at higher radius there is still a noticeable abundance of lasing ions and thus amplification. The result is that this central region impacts both the intensity and phase profiles.

For example, figure 6 shows the radial phase (left) and intensity (right) profile of an amplified high order harmonic when the plasma waveguide has only one overionized region at different positions in the amplifier: initial (upper panels) and central (lower panels). When only the initial overionized region is present, the intensity radial profile (upper right panel) is the one expected if only the lasing ion abundance was taken into account: a central region dominated by the parabolic profile of the plasma waveguide and Gaussian wings mimicking the radial decrease of lasing ion (which follows the IR pump radial profile, which is Gaussian). The phase profile, on the contrary, does not show the expected parabolic profile caused by the plasma waveguide shape but has a flat central region, produced by the inverse parabola shaped electron density profile.

The central inhomogeneous region impacts both intensity and phase profiles, as shown in figure 6, lower panels. The reduced amplification only at low radius regions (due to the lack of lasing ions) creates a dip in the intensity profile that cannot be explained by the parabolic profile of the plasma waveguide only. In addition to this, the electron density peak imprints its shape in the phase profile, observing a strong inverse parabolic profile in its central part.

Since the features in phase and intensity profiles depend in the shape of the overionized regions, they provide an excellent method to probe the lasing ion abundance and electron density of plasma waveguides, unveiling the shape of these inhomogeneities.

It is worth mentioning that the propagation and amplification of the seeded HOH beam is not only affected by these electron density and lasing ion inhomogeneities but also by the propagation velocity mismatch between the IR pump pulse and the HOH. In the experimental configuration, the IR pump beam propagates through the plasma channel, creating the gain that lasts several hundreds of femtoseconds. The HOH is seeded with some optimized delay. This is

the case shown in figure 7 left panel. The HOH seed (in false color) is always matching the gain (grayscale) since both, IR pump beam (and consequently gain) and HOH seed propagate at the same velocity.

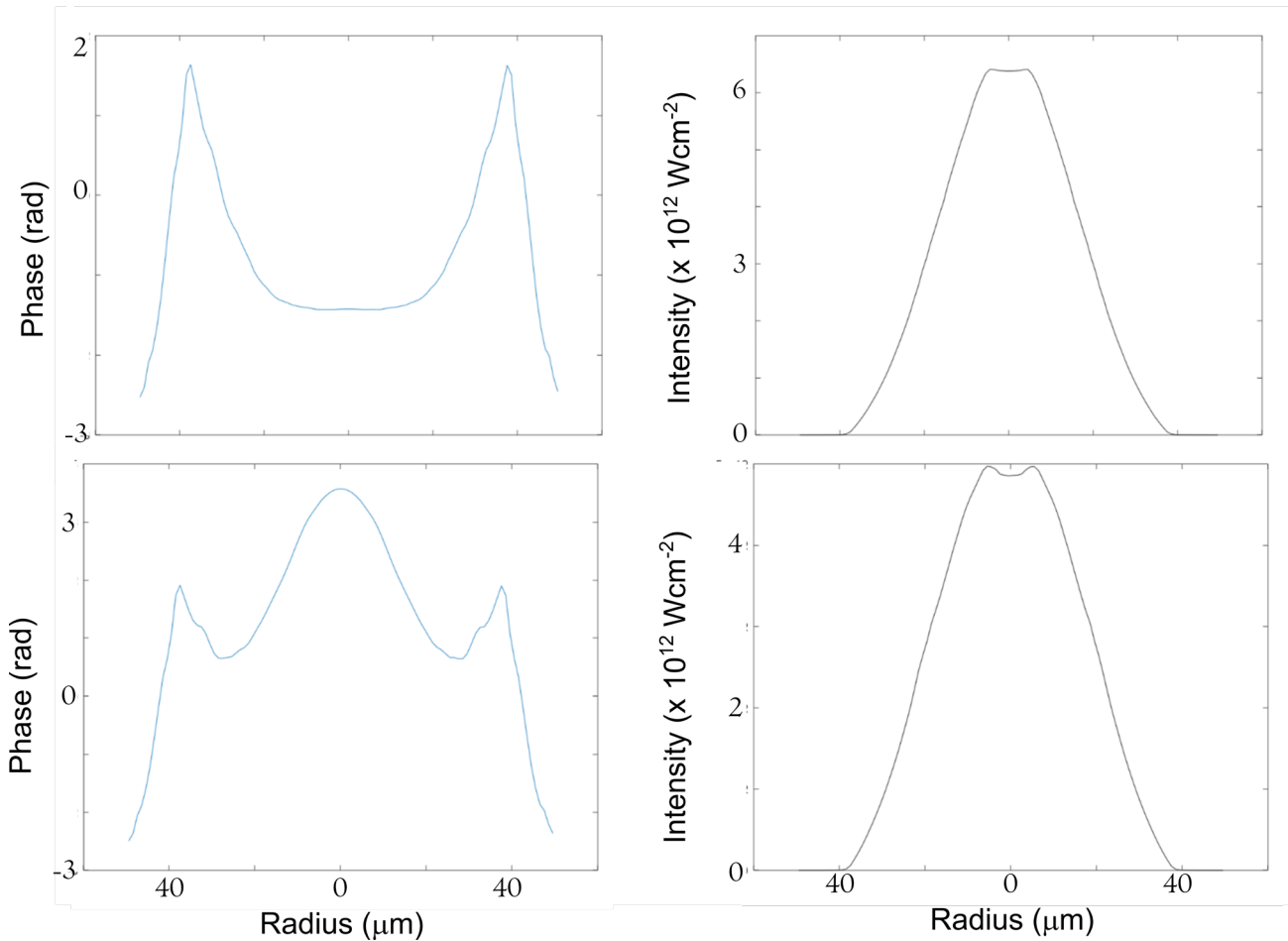


Figure 6. Phase (left) and intensity (right) radial profiles of an amplified high order harmonic when seeded in an inhomogeneous plasma waveguide with one overionized region at the entrance (upper panels) and at the central part (lower panels).

However, since the electron density in the channel is of the order of 10% the critical density of the IR pump pulse, it propagates with a velocity slightly lower than that of the HOH. Thus, the delay between the IR pump pulse and the HOH seed is being reduced along the amplifier and, at some point, the HOH overtakes the IR pump pulse and the gain region. The head of the HOH beam is no longer amplified and it is the tail that is in the gain region. The resulting beam has a slightly longer duration than the gain profile and a complex spatio-temporal profile, as depicted in figure 7 right panel.

4. CONCLUSIONS

In this paper we have presented the modelling framework we use to study plasma based seeded soft X-ray lasers (see also Sect. 2 [31]). The full modelling of these amplifiers is a multiphysics and multiscale problem that requires the coupling of different codes. Plasma hydrodynamics is modelled using the 2D radiative hydrodynamics code ARWEN. Propagation of intense IR pulses in plasmas is modelled using Particle-In-Cell codes, like WAKE-EP and FBPIC. The collisional-radiative code OFIKinRad is used to compute collisional excitation and deexcitation rates, ion abundances, level populations, etc...

Finally, the amplification of high order harmonics is computed with Maxwell-Bloch models, 1D-DeepOne and 3D Dagon.

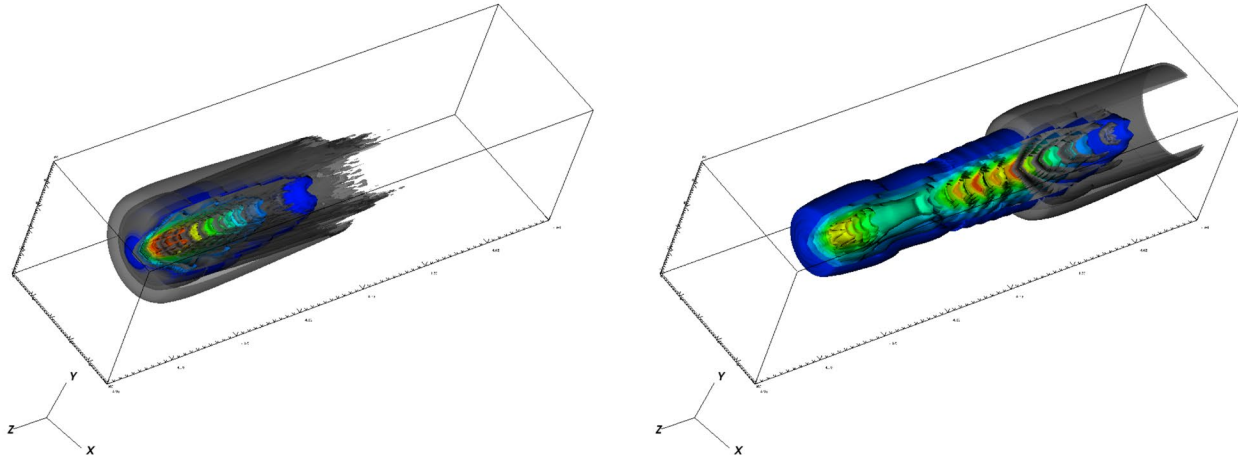


Figure 7. HOH seed beam intensity (false color) and gain (grayscale) when the IR pump pulse and HOH propagate at the same velocity (left) and when the reduced group velocity of the IR pump pulse is taken into account (right).

This framework has been applied to study an optical field ionized dense plasma amplifier seeded by high order harmonics. The plasma has an increasing radial parabolic profile that acts as a waveguide to ease the propagation of the intense IR pump pulse. The resulting amplifier presents inhomogeneities in lasing ion abundance and electron density that impact the intensity and phase profile of the amplified beam. Since these profiles can be measured experimentally, it is a promising method to diagnose the plasma.

ACKNOWLEDGEMENTS

The authors acknowledge support from the European Community's Horizon 2020 research and innovation program under grant agreement 665207, project VOXEL, the Universidad Politécnica de Madrid (UPM), project DERKETA, the Comunidad de Madrid and UPM, línea de actuación estímulo a la investigación de jóvenes doctores, project CROM and the Spanish Ministerio de Ciencia e Innovación through a Ramón y Cajal RYC2018-026238-I fellowship.

REFERENCES

- [1] Matthews, D.L., Hagelstein, P.L., Rosen, M.D., Eckart, M.J., Ceglio, N.M., Hazi, A.U., Meddecki, H., MacGowan, B.J., Trebes, J.E., Whitten, B.L., Campbell, E.M., Hatcher, C.W., Hawryluk, A.M., Kauffman, R.L., Pleasance, L.D., Rambach, G., Scofield, J.H., Stone, G., and Weaver, T.A., “Demonstration of a Soft X-Ray Amplifier”, *Phys. Rev. Lett.* 54, 110 (1985)
- [2] Suckewer, S., Skinner, C.H., Milchberg, H., Keane, C., and Voorhees, D., “Amplification of stimulated soft x-ray emission in a confined plasma column”, *Phys. Rev. Lett.* 55, 1753 (1985)
- [3] Rus, B., Mocek, T., Präg, A. R., Kozlova, M., Jamelot, G., Carillon, A., Ros, D., Joyeux, D., and Phalippou, D., “Multimillijoule, highly coherent x-ray laser at 21 nm operating in deep saturation through double-pass amplification”, *Phys. Rev. A* 66, 063806 (2002)
- [4] Nickles, P.V., Shlyaptsev, V.N., Kalachnikov, M., Schnürer, M., Will, I., and Sandner, W., “Short Pulse X-Ray Laser at 32.6 nm Based on Transient Gain in Ne-like Titanium”, *Phys. Rev. Lett.* 78, 2748 (1997)

- [5] Keenan, R., Dunn, J., Patel, P.K., Price, D.F., Smith, R.F., and Shlyaptsev, V.N., “High-Repetition-Rate Grazing-Incidence Pumped X-Ray Laser Operating at 18.9 nm”, *Phys. Rev. Lett.* 94, 103901 (2005)
- [6] Sebban, S., Haroutunian, R., Balcou, Ph., Grillon, G., Rousse, A., Kazamias, S., Marin, T., Rousseau, J.P., Notebaert, L., Pittman, M., Chambaret, J.P., Antonetti, A., Hulin, D., Ros, D., Kilsnick, A., Carillon, A., Jaeglé, P., Jamelot, G., and Wyart, J.F., “Saturated Amplification of a Collisionally Pumped Optical-Field-Ionization Soft X-Ray Laser at 41.8 nm”, *Phys. Rev. Lett.* 86, 3004 (2001)
- [7] Zeitoun, Ph., Faivre, G., Sebban, S., Mocek, T., Hallou, A., Fajardo, M., Aubert, D., Balcou, Ph., Burgy, F., Douillet, D., Kazamias, S., de Lachèze-Murel, G., Lefrou, T., le Pape, S., Mercère, P., Merdji, H., Morlens, A. S., Rousseau, J.P., and Valentin, C., “A high-intensity highly coherent soft X-ray femtosecond laser seeded by a high harmonic beam”, *Nature* 431, 426-429 (2004)
- [8] Wang, Y., Granados, E., Pedaci, F., Alessi, D., Luther, B., Berrill, M., and Rocca, J.J., “Phase-coherent, injection-seeded, table-top soft-X-ray lasers at 18.9 nm and 13.9 nm”, *Nature Photonics* 2, 94-98 (2008)
- [9] Guilbaud, O., Cojocaru, G.V., Li, L., Delmas, O., Ungureanu, R.G., Banici, R.A., Kazamias, S., Cassou, K., Neveu, O., Demailly, J., Baynard, E., Pittman, M., Le Mareck, A., Klisnick, A., Zeitoun, Ph., Ursescu, D., and Ros, D., “Gain dynamics in quickly ionized plasma for seeded operated soft x-ray lasers”, *Opt. Lett.* 40, 4775 (2015)
- [10] Depresseux, A., Oliva, E., Gautier, J., Tissandier, F., Nejdil, J., Kozlova, M., Maynard, G., Goddet, J.P., Tafzi, A., Lifschitz, A., Kim, H.T., Jacquemot, S., Malka, V., Ta Phuoc, K., Thaury, C., Rousseau, P., Iaquaniello, G., Lefrou, T., Flacco, A., Vodungbo, B., Lambert, G., Rousse, A., Zeitoun, Ph., and Sebban, S., “Table-top femtosecond soft X-ray laser by collisional ionization gating”, *Nature Photonics* 9, 817-821 (2015)
- [11] Oliva, E., Fajardo, M., Li, L., Pittman, M., Le, T.T.T., Gautier, J., Lambert, G., Velarde, P., Ros, D., Sebban, S., and Zeitoun, Ph., “A proposal for multi-tens of GW fully coherent femtosecond soft X-ray lasers”, *Nature Photonics* 6, 764-767 (2012)
- [12] Oliva, E., Fajardo, M., Li, L., Sebban, S., Ros, D., and Zeitoun, Ph., “Soft X-ray plasma-based seeded multistage amplification chain”, *Opt. Lett.* 37, 4341-4343 (2012)
- [13] Wang, Y., Wang, S., Oliva, E., Li, L., Berrill, M., Yin, L., Nejdil, J., Luther, B., Proux, C., Le, T.T.T., Dunn, J., Ros, D., Zeitoun, Ph., and Rocca, J.J., “Gain dynamics in a soft-X-ray laser amplifier perturbed by a strong injected X-ray field”, *Nature Photonics* 8, 381-384 (2014)
- [14] Depresseux, A., Oliva, E., Gautier, J., Tissandier, F., Lambert, G., Vodungbo, B., Goddet, J.P., Tafzi, A., Nejdil, J., Kozlova, M., Maynard, G., Kim, H.T., Ta Phuoc, K., Rousse, A., Zeitoun, Ph., and Sebban, S., “Demonstration of a circularly polarized plasma-based soft-X-ray laser”, *Phys. Rev. Lett.* 115, 083901 (2015)
- [15] Tuitje, F., Martínez Gil, P., Helk, T., Gautier, J., Tissandier, F., Goddet, J.P., Guggenmos, A., Kleineberg, U., Sebban, S., Oliva, E., Spielmann, C., and Züch, M., “Nonlinear ionization dynamics of hot dense plasma observed in a laser-plasma amplifier”, *Light:Science & Applications* 9 (2020)
- [16] Ogando, F., and Velarde, P., “Development of a radiation transport fluid dynamic code under AMR scheme”, *J. Quant. Spectrosc. Rad. Transf.* 71, 541-550 (2001)
- [17] Cotel, M., Velarde, P., de la Varga, A.G., Portillo, D., Stehlé, C., Chaulagain, U., Kozlova, M., Larour, J., and Suzuki-Vidal, F., “Simulation of radiative shock waves in Xe of last PALS experiments”, *High Ener. Dens. Phys.* 17, 68-73 (2015)
- [18] Mora, P., and Antonsen, T., “Kinetic modeling of intense, short laser pulses propagating in tenuous plasmas”, *Phys. Plasmas* 4 (1997)
- [19] Paradkar, B. S., Cros, B., Mora, P., and Maynard, G., “Numerical modelling of multi-GeV laser wakefield electron acceleration inside a dielectric capillary tube”, *Phys. Plasmas* 20, 083120 (2013)
- [20] Lehe, R., Kirchen, M., Andriyash, I., Godfrey, B., and Vay, J.L., “A spectral, quasi-cylindrical and dispersion-free Particle-In-Cell algorithm”, *Comp. Phys. Comm.* 203, 66-82 (2016)
- [21] Cros, B., Mocek, T., Bettaibi, I., Vieux, G., Farinet, M., Dubau, J., Sebban, S., and Maynard, G., “Characterization of the collisionally pumped optical-field-ionized soft-x-ray laser at 41.8 nm driven in capillary tubes”, *Phys. Rev. A* 73, 033801 (2006)
- [22] Oliva, E., Zeitoun, Ph., Fajardo, M., Lambert, G., Ros, D., Sebban, S., and Velarde, P., “Comparison of natural and forced amplification regimes in plasma-based soft-x-ray lasers seeded by high-order harmonics”, *Phys. Rev. A* 84, 013811 (2011)
- [23] Oliva, E., Cotel, M., Escudero, J.C., González-Fernández, A., Sanchis, A., Vera, J., Vicéns, S., and Velarde, P., “Dagon: a 3D Maxwell-Bloch code”, *Proc. SPIE* 10243, 1024303 (2017)

- [24] Durfee, C.G., and Milchberg, H.M., “Light pipe for high intensity laser pulses”, Phys. Rev. Lett. 71, 2409 (1993)
- [25] Oliva, E., Depresseux, A., Tissandier, F., Gautier, J., Sebban, S., and Maynard, G., “Self-regulated propagation of intense infrared pulses in elongated soft-x-ray plasma amplifiers”, Phys. Rev. A 92, 023848 (2015)
- [26] Oliva, E., Depresseux, A., Cotelo, M., Lifschitz, A., Tissandier, F., Gautier, J., Maynard, G., Velarde, P., and Sebban, S., “Hydrodynamic evolution of plasma waveguides for soft-x-ray amplifiers”, Phys. Rev. E 97, 023203 (2018)
- [27] “Block-Structured AMR Software Framework and Applications”, < <https://amrex-codes.github.io/>> (January 2021)
- [28] More, R.M., Warren, K.H., Young, D.A., and Zimmerman, G.B., “A new quotidian equation of state (QEOS) for hot dense matter”, Phys. Fluids 31, 3059-3078 (1988)
- [29] De la Varga, A.G., Velarde, P., Cotelo, M., de Gaufridy, F., and Zeitoun, Ph., “Radiative properties for warm and hot dense matter”, High Ener. Dens. Phys. 7, 163-168 (2011)
- [30] De la Varga, A.G., Velarde, P., de Gaufridy, F., Portillo, D., Cotelo, M., Barbas, A., González, A., and Zeitoun, Ph., “Non-Maxwellian electron distributions in time-dependent simulations of low-Z materials illuminated by a high-intensity X-ray laser”, High Ener. Dens. Phys. 9, 542-547 (2013)
- [31] D. Bleiner, The Science and Technology of X-ray Lasers: A 2020 Update Proc. SPIE 11886, 1188602 (2021)